

Numerical Simulation of Swirl and Methane Equivalence Ratio Effects on Premixed Turbulent Flames and NOx Apparitions

S. Ouali^{1†}, A. H. Bentebbiche² and T. Belmrabet³

¹*Energetic Department, Faculty of Engineering UMBB, Boumerdes, 35000, Algeria*

²*Energy Systems Laboratory, Faculty of Mechanic, USTHB, Algiers, 16111, Algeria*

³*Military Polytechnic Academy, EMP, Algiers, 16000, Algeria*

†*Corresponding Author Email: sofianeouali2@hotmail.fr*

(Received December 24, 2013; accepted April 15, 2015)

ABSTRACT

This paper presents a three dimensional numerical simulation of premixed methane-air low swirl stabilized flames. The computational domain has a simple geometry describing a LBS (low swirl burner) with 50mm of nozzle diameter. RANS Standard $\kappa - \epsilon$ model to treat turbulence coupled with partially premixed combustion model are used. The purpose is to show the applicability limits and their capacities to predict governing flame parameters by varying swirl intensity and CH₄ mass fraction at the inlet, which shows the optimum operating area of the burner in terms of generated energy and flame stability with a particular interest to thermal NO_x apparitions. This work is compared and validated with experimental and LES numerical simulation works available in the literature. Results offered good similarity for all flame studied parameters. Swirl number was varied from 0.5 to 1.0 to ensure a wide operating range of the burner. From $S=0.6$, we observed the onset of recirculation zones, while for the inert flow the appearance of recirculation zones was observed for $S=0.9$. CH₄ equivalence ratio was increased from 0.6 to 1.4. That showed apparition of zones with important NO_x mass fraction due to the existence of zones with high temperature. Otherwise, the flow field wasn't disturbed in terms of recirculation zones apparitions who remained absent for all cases. Actual investigation works to find equilibrium between the maximum of generated temperature and the minimum of NO_x emissions for swirled burners. Used models haven't showed applicability limits, results were clear and precise and offered a significantly gain in computing time and means.

Keywords: Turbulence; Premixed combustion; Methane-air; Recirculation zones; Flame stability; Pollutants; swirl.

NOMENCLATURE

\bar{c}	mean reaction progress variable	S	swirl number
D	burner nozzle diameter	Sch_t	turbulent Schmidt number
D_h	hydraulic diameter	Sch	Schmidt number
HSB	high swirl burner	Sc	reaction progress source term
I	turbulent intensity	V_{ax}	axial velocity
LSB	low swirl burner	V_{rad}	radial velocity
PDF	probability density function	V_s	swirl velocity
Pr	Prandtl number	V_0	initial velocity
Re	Reynolds number	Φ	equivalence ration of CH ₄

1. INTRODUCTION

The premixed swirling flames have a very wide range

of applications in modern devices such as gas turbines, industrial burners and several types of combustion process.

Swirl burners bring an important technique to stabilize the flame, reduce NOx emissions and avoid intrusive methods disturbing flow field.

In the beginning, this method generated a large zone of recirculation (vortex) where it traps hot combustion products who continuously ignites fresh mixtures, thus increase zones of high temperature including most important of NOx apparitions. The flame was stabilized close to the nozzle burner walls what generates a premature degradation of the burner structure. This case was called high swirl burner (HSB). Currently, the challenge of scientist is to minimize apparition of recirculation zones while keeping advantages of swirl stabilization methods. That directed researches to develop burners with same operating conditions by reducing swirl factor and changing several parameters; burner geometry, reduce diameter of the annular space including swirl vanes, find the optimum of swirl intensity, propose the most suitable equivalent ratio and many others techniques. This case is called low swirl burner (LSB).

Actual study is interested by flame behavior according to swirl intensity and CH₄ equivalence ratio increasing.

Flow field, thermal field and NOx apparition are analyzed using commercial code ANSYS Fluent 14.5 with RANS Standard κ - ϵ model to treat turbulence coupling to Partially Premixed model to treat combustion. Models are applied to a three dimensional geometry and gave suitable results. Vortexes were nonexistent for all CH₄ equivalence ratios studied, when thermal field were according to this increase. However, for swirl intensity study, the appearance of recirculation zones is observed from $S = 0.6$, whereas, for inert cases, their appearances starting to $S = 0.9$, this compromise between CH₄ equivalence ration and swirl intensity allowed us to undertake this study.

Several works are interested by low swirl burners to decrease pollutants apparitions, stabilize flame front create and to create a database validation for different existing models.

At the beginning, low swirl burner technology started with Cheng, R.K. (1995). He proposed a low-swirl flame stabilization method in 1991 to study the dynamic and chaotic interactions between turbulent flow and premixed combustion. The results showed significant pollutants emissions reduction (thermal NO) and a new flame stabilization method. Currently, several scientist works in this axis; Plessing, T. *et al* (2000) have developed an experimental study where they interested to measure the turbulent burning velocity and the structure of premixed flames on a LSB using PIV. They found that LSB allows stabilization of planar flames without heat losses or boundary effects. Bell, J.B. *et al* (2002), studied the behavior of a premixed turbulent methane flames in three dimensions using numerical simulation at low Mach number, they found that the variation levels of

turbulent intensity show increased flame area and enhancement of the laminar flame speed.

Johnsona, M.R. *et al* (2005) developed a study where they compares flow fields and burners emissions to high swirl number of HSB and LSB, they concluded that the two configurations have similar operating ranges and the flow generated by the LSB is devoid of a large dominant strong recirculation zone contrary to HSB kind. Huang, Y. and V. Yang (2005) have undertaken a numerical simulation of swirl effect on combustion dynamics in lean premixed swirl stabilized combustion where they found that the inlet swirl number increases with upstream displacement of the central recirculation zone and higher swirl number resulting in an increase of the turbulence intensity of flame speed. Cheng, T.S. *et al* (2006) examined multipoint measurements of flame emission spectra using two Cassegrain mirrors and two spectrometers, they used results to obtain the correlation of the intensity ratios to the equivalence ratio in the laminar flames. Bell, J.B. *et al* (2007) studied a numerical simulation of Lewis number effect of lean premixed turbulent flames where they showed that the local burning rate for methane flames is more insensitive to the flame curvature.

Pfadler, *Set al* (2007) studied experimentally the turbulent flux in turbulent premixed swirl flames. Galpin, J., *et al* (2008) executed a LES numerical simulation of a fuel in lean premixed turbulent swirling flame in the configuration of a burner experimentally studied where they proposed that some models improvements will need to be considered. Nogenmyr, K.J. *et al* (2009) proposed an LES numerical simulation about Cheng, R.K. (1995) configuration burner for the turbulent premixed methane-air flames and published a study where they changed the calculation source term in the G-equation combustion model and compared it with TFC model and his own experiences. They found that the G-LES model properly reproduces the thin reaction zone behavior and the F-LES predicts a thicker fuel consumption zone and less degree of wrinkling. Littlejohn, D. *et al* (2010) studied LSB compartment with adding hydrogen. Petersson, P. *et al* (2012) have developed an experimental study about high speed measurements using PIV and OH PLIF and they analyzed flame models for of a LSB burner. Their results showed that vortices in the outer flame region create a local flow reversal flow and thus contribute to improve large-scale mixing of reactants.

2. NUMERICAL SIMULATION AND MATHEMATICAL FORMULATION

Reactive flows are governed by fluid mechanics equations coupled with those of aerothermochemistry. According to used models, following averaged equations are needed to resolve studied phenomena according to ANSYS Fluent 14.5

(2012) guide theory.

Mass conservation equation

$$\frac{\partial(\rho u_i)}{\partial x_j} = 0 \quad (1)$$

Momentum equation

$$\frac{\partial}{\partial x_j}(\rho u_i u_j) = \frac{\partial P}{\partial x_j} + \frac{\partial \tau_{ij}}{\partial x_j} + \rho F_i + \frac{\partial}{\partial x_j}(-\rho u_i' u_j') \quad (2)$$

Energy equation

$$U_j \frac{\partial U_i}{\partial x_j} = -\frac{\partial}{\partial x_i} \left(\frac{P}{\rho} \right) + \frac{\partial}{\partial x_j} \left(\nu \frac{\partial U_i}{\partial x_j} - \overline{u_i u_j} \right) \quad (3)$$

State equation

$$p = \rho RT \sum_i \frac{Y_i}{W_i} \quad (4)$$

Conservation equation of chemical species

$$\frac{\partial(\rho Y_k)}{\partial t} + \frac{\partial(\rho u_i Y_k)}{\partial x_j} = \frac{\partial(J_j^k)}{\partial x_j} + \dot{\omega}_k \quad (5)$$

$$J_j^k = -\rho D_k \frac{\partial(Y_k)}{\partial x_j} \quad (6)$$

RANS Standard $\kappa - \varepsilon$ turbulence model (Lauder, B.E. and D.B. Spalding (1972)) is based on two equations, it can determine the length of turbulence and the time scale independently by solving two transport equations.

It is based on models of transport equations for the turbulence kinetic energy (κ) and its dissipation rate (ε). The transport model equation is derived from the exact equation, while the model transport equation for ε is obtained using physical deduction.

Transport equation where κ and ε are obtained from:

$$\frac{\partial}{\partial t}(\rho \kappa) + \frac{\partial}{\partial x_i}(\rho \kappa u_i) = \frac{\partial}{\partial x_j} \left[\left(\mu + \frac{\mu_t}{\sigma_k} \right) \frac{\partial \kappa}{\partial x_j} \right]$$

$$+ G_k + G_b - \rho \varepsilon - Y_M + S_k \quad (7)$$

In addition:

$$\frac{\partial}{\partial t}(\rho \varepsilon) + \frac{\partial}{\partial x_i}(\rho \varepsilon u_i) = \frac{\partial}{\partial x_j} \left[\left(\mu + \frac{\mu_t}{\sigma_\varepsilon} \right) \frac{\partial \varepsilon}{\partial x_j} \right]$$

$$+ C_{1\varepsilon} \frac{\varepsilon}{\kappa} (G_k + C_{3k} G_b) - C_{2\varepsilon} \rho \frac{\varepsilon^2}{\kappa} + S_\varepsilon \quad (8)$$

The eddy viscosity is obtained by combining κ and ε by:

$$\mu_t = \rho C_\mu \frac{\kappa^2}{\varepsilon} \quad (9)$$

Model constants are:

$$C_{1\varepsilon}=1.44, C_{2\varepsilon}=1.92, C_\mu=0.09, \sigma_k=1.0, \sigma_\varepsilon=1.3.$$

Partially premixed model is a form of premixed flames model with non-uniform fuel-oxidizer mixtures. We used Zimont model for calculating turbulent flame speed (Zimont, V. 2000; Zimont, V. *et al* 1998; Zimont, V.L. and A.N. Lipatnikov 1995), TFC model for premixed flame and a PDF (Pope S.B. (1985) for turbulence chemistry coupling who calculates a progress variable c considering the 13 chemical species in chemical equilibrium. The chemical species transport equation is given by:

$$\frac{\partial}{\partial t}(\rho \bar{c}) + \nabla \cdot (\rho \bar{v} \bar{c}) = \nabla \cdot \left(\frac{\mu_t}{Sc_t} \nabla \bar{c} \right) + \rho S_c \quad (10)$$

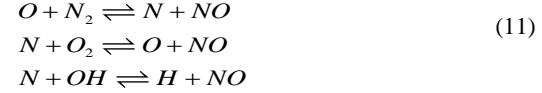
With:

$c = 0$; unburned mixture.

$c = 1$; burned mixture.

Using thermal NO model, additional equations are injected into the equation of chemical species conservation and the thermal NO formation is determined by a series of chemical reactions which depend strongly on the temperature which is known as the Zeldovich mechanism (Flower, W.L. *et al* (1975), Blauvens, J. *et al* (1977), Monat, J.P. *et al* (1979)).

The equations of the system are reduced as follows:



3 GEOMETRY AND VALIDATION

Obtained results are validated with experiments and LES numerical simulation data of K.-J. Nogenmyr and all (2009), which is only the improving of the burner structure proposed by Robert Cheng (1995).



Fig. 1. LSB burner configuration.

Figure 1 shows the LSB structure of the burner proposed by Cheng, R.K. (1995). The inclination

angle of swirler vales α define swirl intensity S represented by the tangential velocity. The perforated plate represents the adjustment of the position of walls where the mixture of methane-air is injected.

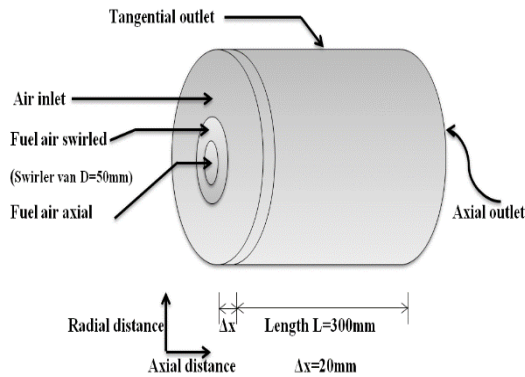


Fig. 2. Computational domain configuration.

Figure 2 shows the computational domain (3D). The geometry of the volume is simple and open to atmospheric pressure. The flame is stabilized by a swirl, the burner consists of a nozzle $D = 50\text{mm}$ diameter divided into two parts, axial perforated plate of 30mm diameter where the flow is purely axial and an annular space which forms the valve swirler of 20mm diameter with co-current flow of air surrounding this nozzle.

3.1 Mesh and Grid Refinement

Adopted mesh is structured no uniform refined in zones with important gradient of velocity, temperature and turbulence so it was refined near the nozzle in the axial and radial distance.

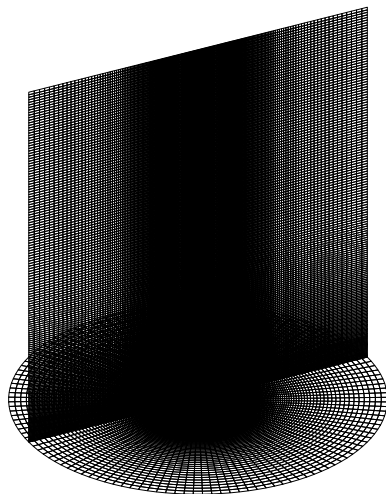


Fig. 3. Overall view of the mesh structure for the radial and axial sections.

Figure 3 shows the refinement of the mesh grid near the nozzle in the axial and radial distance. The refinement coincides with zones of high velocity and temperature gradient. Several cases were simulated

for different nodes number; the numerical simulation began with 83700 nodes then 1209000, 1570000, 1950000 and finally 3400000 nodes.

Axial temperature profiles for different nodes number are shown in the following figure:

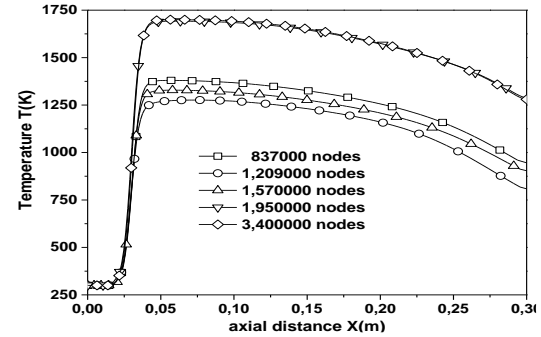


Fig. 4. Temperature profiles along the axis X for different nodes numbers of mesh.

Figure 4 shows an independence of the solution from 1950000 nodes justifying our choice of this configuration.

3.2 Boundary and Operating Conditions

The flow is considered permanent and incompressible. Using ANSYS Fluent 14.5, we employed the Pressure-Based solver (Chorin, A.J. 1968) which is an algorithm that belongs to a general class of methods called projection method and SIMPLEC scheme (proposed by Vandoormaal, J.P and G.D. Raithby 1984) with second order solver algorithms pressure based available as an isolated algorithm.

Table 1 Operating conditions

Solver	Pressure based
Operating pressure	1 ATM
Equivalence ratio Φ of CH ₄	0.6-0.8-1-1.2-1.4
Swirl number S	0.5-0.6-0.7-0.8-0.9-1.0
Inlet temperature T	300°K
Swirl number S	~0.5
Reynolds Re	11400
Inlet velocity V_0	~5m/s
Turbulent Schmidt	0.5
Prandtl Pr	0.85
PDF Schmidt number	0.85

Table 1 summarizes the parameters used for this study. Actual work is composed of two parts; the CH₄ equivalence ratio effect (varied from 0.6 to 1.4) and swirl intensity effect (varied from 0.5 to 1.0). the flow of methane-air mixture passes through two separate parts, the perforated plate and the annular swirled space, both constitute the structure of the burner

nozzle, two boundary conditions have been fixed;

1. Methane - air in the axial perforated plate

This section is situated in the axial part of the nozzle, where a purely axial velocity of premixed methane-air is posed to reduce overall velocity and turbulence of the flow, different parameters are posed in the following table:

Table 2 Boundary conditions at the axial perforated plate

V _{ax} (m/s)	V _{rad} (m/s)	V _s (m/s)	I (%)	Dh (mm)
1.785	0	0	12	30

2. Methane - air in the annular swirled space

In this section, the mixture of methane-air through an annular space surrounding the axial perforated plate, which defines the swirler burner valve with I = 12 % and Dh = 32 mm.

V_s is obtained by:

$$V_s = V_{ax} * \tan \alpha \quad (12)$$

In accordance with Cheng, R.K. (1995), Nogenmyr K.J. *et al* (2009) and Pesenti, B. (2006).

Where α is the inclination angle of the swirler vanes. The vanes can have a constant angle of inclination or variable that does not affect the parameters set in the numerical simulation in accordance with Cheng, R.K. (1995).

The swirl number S is defined by:

$$S = (2/3) * \tan \alpha \left(\frac{1 - R^3}{1 - R^2 \left[m^2 (1/R^2 - 1)^2 \right] R^2} \right) \quad (13)$$

In agreement with Cheng, R.K. (1995) and Nogenmyr, K.J. *et al* (2009).

Where R is the ratio between the radius of the central duct and the radius of the nozzle burner and the m is the rate between the mass flow passing through the central plate and the mass flow passing through the annular swirled space.

3. The air surrounding the burner nozzle

The boundary conditions of the air were set 20mm upstream of the burner nozzle section; the different posed parameters are as following:

Table 3 Boundary conditions (c)

V _{ax} (m/s)	V _{rad} (m/s)	V _s (m/s)	I (%)	Dh (mm)	O2 mass fraction
0.3	0	0	0.1	125	0.23

4. Axial outlet of the computational volume

This part is supposed far than the nozzle and the flow

through from this section.

5. Tangential outlet of the computational domain

This area borders the computing domain radially and assumed far then the perturbations caused by the flame, a symmetry condition was posed.

For CH4 equivalence ratio effect, table 4 summarize different fuel-oxidant compositions in the perforated plate and the annular swirled space:

Table 4 Mixture composition for CH4 equivalence ratio effect

Case	CH4 Equivalence ratio	Mixture composition		
		CH4 mass fraction	O2 mass fraction	N2 mass fraction
1	0.6	0.0348	0.22	0.7452
2	0.8	0.044	0.215	0.741
3	1	0.05482	0.21	0.73518
4	1.2	0.065	0.205	0.73
5	1.4	0.0754	0.20	0.7246

For swirl intensity study, table 5 summarize different inlets velocities imposed at the annular swirled space:

Table 5 Velocities distribution at the annular space for swirl intensity study

Case	Swirl number S	V _{ax} (m/s)	V _s (m/s)
1	S=0.5	3.8	2.85
2	S=0.6	3.525	3.17
3	S=0.7	3.265	3.44
4	S=0.8	3.025	3.66
5	S=0.9	2.825	3.817
6	S=1.0	2.625	3.96

3.3 Temperature Profiles Validation

Temperature profiles along the axis X of the burner were obtained by adjusting several numerical simulation parameters cited and the results are satisfying.

Figure 5 shows great similarities between the present work and Nogenmyr, K.J. *et al* (2009) data. The position of the flame front on the axial distance and the maximum of temperature coincide clearly, but its evolution along the axial distance X shows differences between the two numerical simulations. This is certainly due to the combustion model.

3.4 Axial Velocity Profiles Validation

Validation of axial velocity profiles is extremely important. It shows the ability of the used models to predict the velocity field and capture susceptible areas containing vortex, which implies the appearance of zones with high temperature generating significant

NOx emissions.

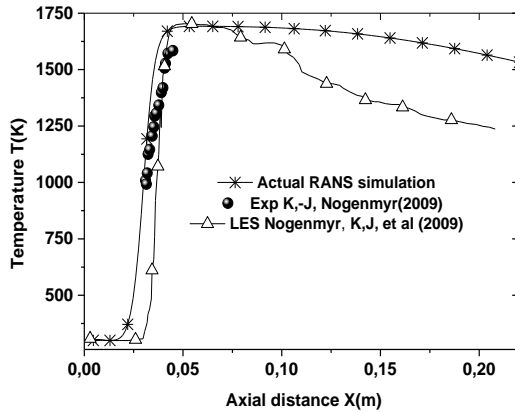


Fig. 5. Validation of temperature profiles along the axial distance X.

Figure 6 shows normalized axial velocities (V_{ax}/V_0) for actual numerical simulation and Nogenmyr, K.J. *et al* (2009) data. For sections $X/D = 0.2, 0.4$ and 0.6 , our results are identical to those of LES simulation taken as reference, but the maximum values are lower than experimental results.

It is noted that for the sections $X/D = 0.8, 1$ and 1.2 , between $R = 0m$ and $0.02m$, axial velocities provided by actual work are overestimated then experimental data but remains acceptable by comparing them with the LES simulation of the same reference. This overestimation is the results of combustion model who neglect endothermic reactions.

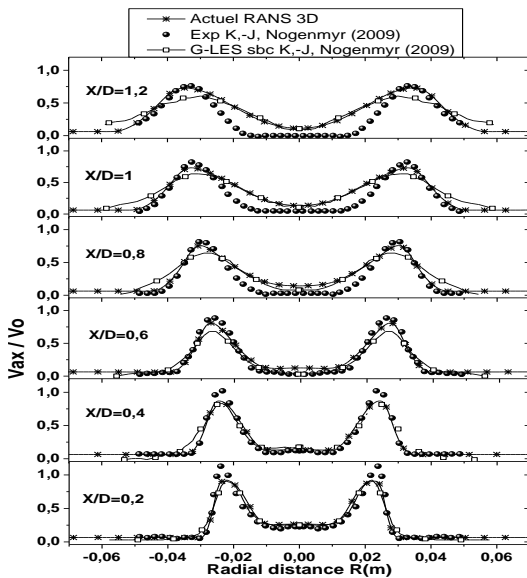


Fig. 6. Axial velocity profiles validation.

3.5 CH4 Distribution Profiles Validation

The choice of combustion model is essential to study

the distribution of chemical species in the flames. According to the results available in the literature, PDF model are among the best choices for its ability to predict chemical species fields according to experiences without neglecting turbulence.

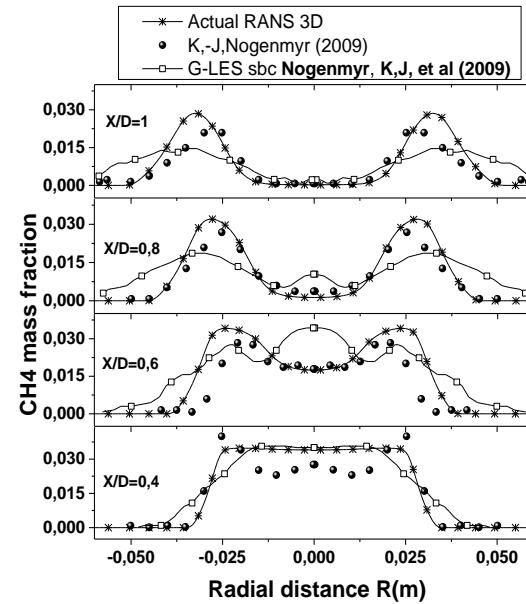


Fig. 7. CH4 mass fraction profiles validation.

The capacity of used models to predict the distribution of CH4 is shown in Fig. 7. Curves show very satisfying results in different sections of the field.

4 RESULTS AND DISCUSSION

The aim of this work is to find an optimum between the CH4 equivalence ratio and the swirl number S . these variations (CH4 equivalence ratio and swirl intensity) are interested by flame structure and NOx apparitions. Parameters governing flames are analyzed in detail (temperature, velocity and NOx).

4.1 The Study of Thermal Field

Figure 8 shows an abrupt increase of temperature, which is a characteristic of combustion process. The increase of CH4 equivalence ratio Φ has involved the development of flame front even closer to the burner walls. This may cause premature degradation of the burner structure. Also, the principle of low swirl stabilization is being questioned (the maintenance of the burner to the inlet temperature of the reactants). On the other hand, the increase of CH4 equivalence ratio ($0.6 < \Phi < 1$) has involved an increase of the reached temperature (from 1680K to 2200K). Whereas for $1 < \Phi$, we observed a decrease of the flame temperature which is due to lack of oxygen in the domain.

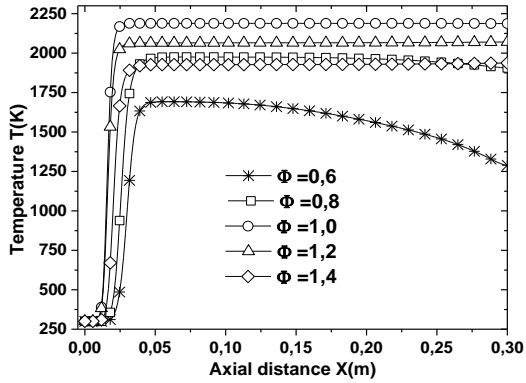


Fig. 8. Temperature profiles for different CH4 equivalence ratios.

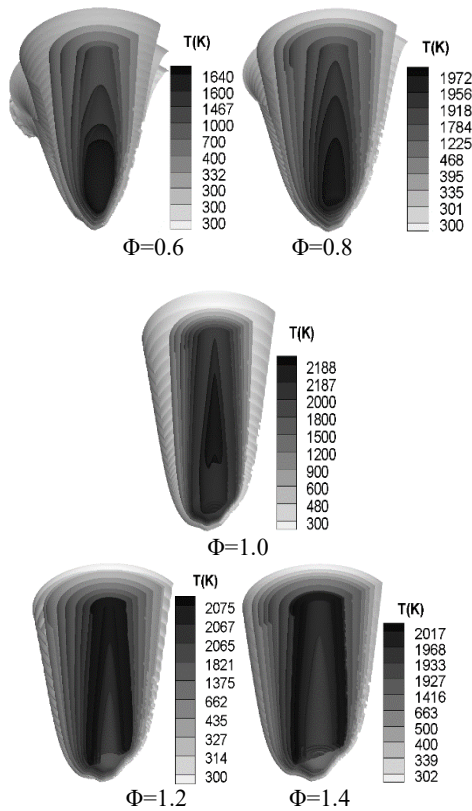


Fig. 9. Temperature iso-surfaces for different CH4 equivalence ratios.

Increasing CH4 equivalence ratio of premixed fuel-air affects the general shape of the flames where flame forms become stretched to the radial distance R and take a larger volume as shown in Fig. 9. This new form of the flame front can disrupt its stability which will be more sensitive to external flow conditions increasing the probability of extinction problems and flashbacks.

This temperature rise will result in a greater occurrence of NOx, which will be presented in the next few curves.

The increase of swirl number from 0.5 to 1.0 has not increased the maximum values of reached temperatures (1670 K). In the axis X of the domain, we remarked that the increase of swirl number implies a decrease of temperature (Fig. 10).

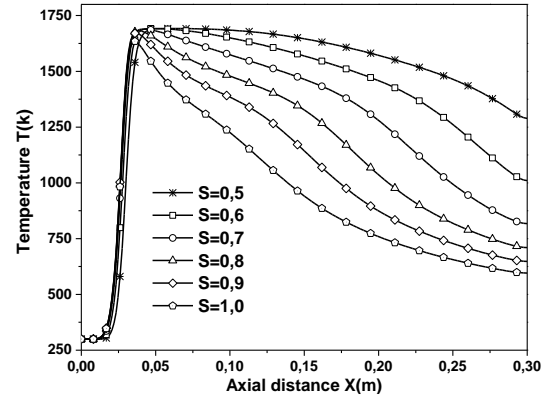


Fig. 10. Temperature profiles for different swirl number.

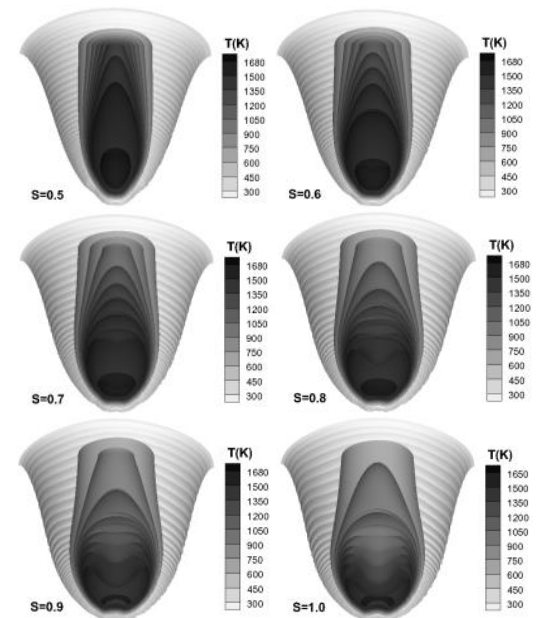


Fig. 11. Temperature iso-surfaces for different swirl number.

The decrease of the temperature on the axis of the field has resulted in a displacement of the latter to the radial distance. Figure 11 shows that increasing the swirl number brings up the flame shape less stretched to the axial distance (shorter) and wider on the radial distance without modification in the maximum of reached temperatures.

4.2 The Study of Velocity Field

Combustion affects greatly the dynamic flow field and redefines a new velocities distribution. From Figure 12, we found that combustion deviated maximums of

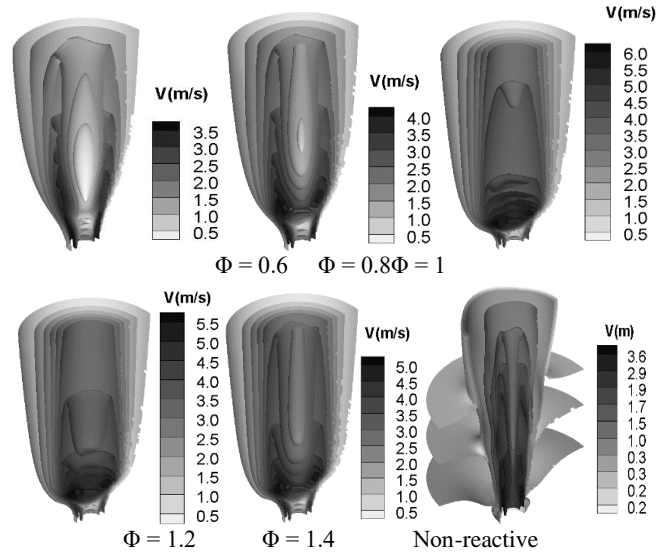


Fig. 13. Axial velocity iso-surfaces for different CH₄ equivalence ratios.

axial velocities to the radial distance R in comparison with the non-reactive case. Axial velocity values are strictly positive, which explains the inexistence of recirculation zones proving again once the particularity of LSB burners.

On section X/D = 0.2, the axial velocity profiles for different CH₄ equivalence ratio haven't shown differences, but they are less important than the non-reactive case, this is explained by the stabilization of the flame in this area where the reaction of methane-air begin.

The axial velocities values increase proportionally with CH₄ equivalence ratio for Φ = 0.6, 0.8 and 1 cases. The maximum axial velocity is raised for Φ = 1 case, which allows to deduce that the axial velocities are proportional to the thermal field.

For Φ = 1.2 and 1.4 cases, axial velocity profiles are less significant compared to the stoichiometric case, which is the result of the temperature decrease. These results showed that the poor case (Φ = 0.6) develops a flame with axial velocity resembling to non-reactive cases which allows a better stabilization of the flame.

Figure 13 shows precisely that the increasing of CH₄ equivalence ratio does not affect apparition of recirculation zones, which provides stabilization of the flame. Nevertheless, its augmentation increases the values of axial velocities redefining larger flames stressing that Φ = 0.6 case offers a similar flow field to the non-reactive case. This leaves us to conclude that increased CH₄ equivalence ratio may cause flame instability.

The variation of swirl number (from 0.5 to 1.0) brings up recirculation zones from S=0.6 (Fig. 14). Axial velocity profiles became become more stretched towards the radial distance R. These recirculation

zones redefine wider and shortcuts flames with a rapprochement to the burner nozzle (temperature on the burner structure increased). The even wider forms of flames become more sensitive to external flow conditions, which increases the risk of extinction and flashback.

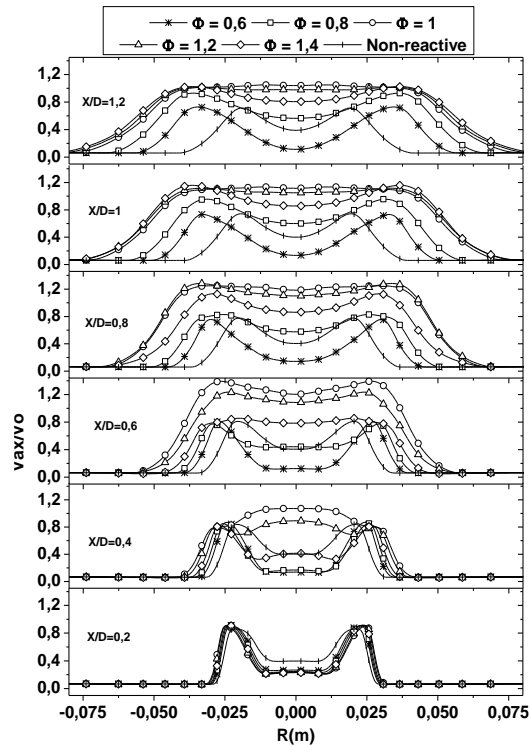


Fig. 12. Axial velocity profiles for different CH₄ equivalence ratios.

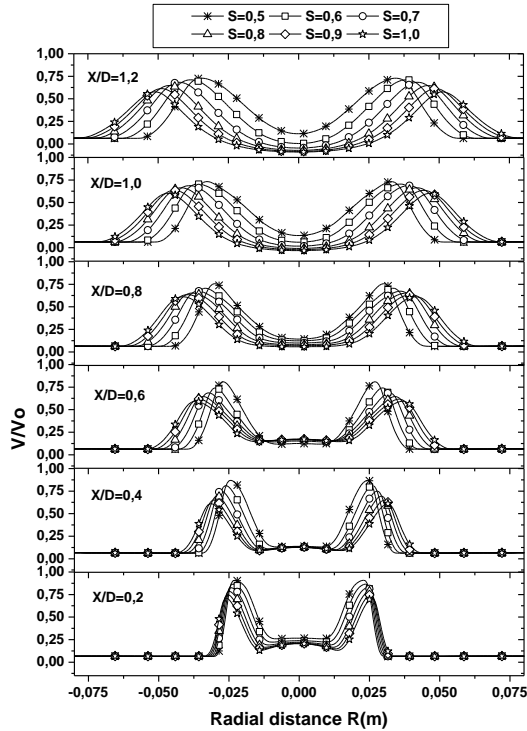


Fig. 14. Axial velocity profiles for different swirl number (reactive).

For non-reactive case, apparition of recirculation zone is noted from $S=0.9$ (Fig. 15). The comparison between the reactive and non-reactive case shows that combustion promotes recirculation zones.

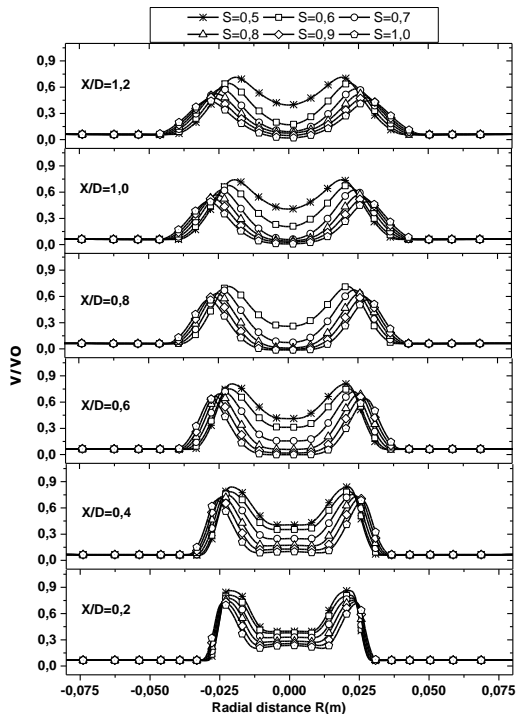


Fig. 15. Axial velocity profiles for different swirl number (non-reactive).

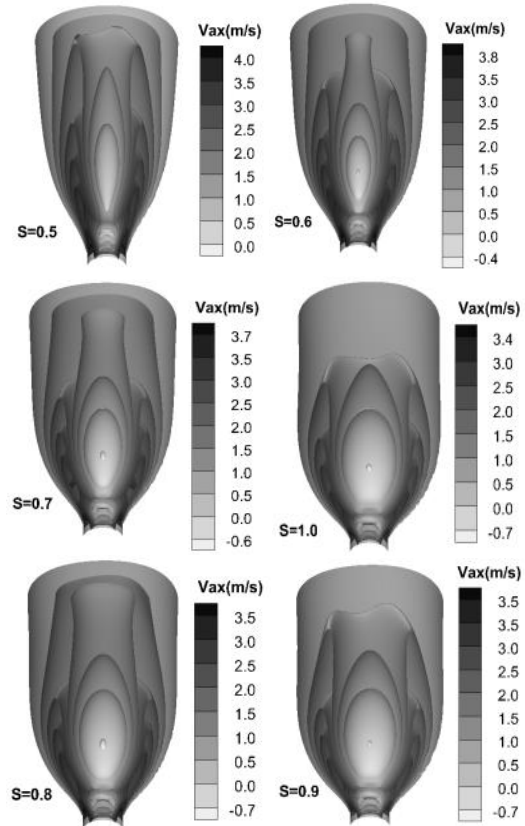


Fig. 16. Axial velocity iso-surfaces for different swirl number.

We notice that the increase in negative values of the axial velocity implies a decrease in maximum positive values reached (Fig. 16).

Recirculation zones observed by increasing swirl intensity did not disturb significantly the flames forms. However, the stabilization became more sensitive.

4.3 The Study of NOx Apparitions

Part of the interest of this study is the appearance of thermal NOx due to the existence of zones with high temperatures.

We notice that the increase of CH4 mass fraction involves the appearance of a larger quantity of NOx due to the temperature (Fig. 17). The premixed methane-air composition does not directly affect its appearance, that is the results of existence of high temperature zones, which explains the decrease of the NOx appearance for $\Phi = 1.2$ and 1.4 .

The comparison between $\Phi = 0.6$ and $\Phi = 1$ shows the appearance of NOx from 0 to 200 ppm.

Figure 18 shows that the NOx apparition depends mainly on developing a high temperature zones. On sections $X/D=0.2$ and 0.4 , we note the absence of pollutants NO for all cases of CH4 equivalence ratio

studied, that is explained by their appearance in areas of high temperature, in this section the flame is just at the beginning. For the rest of sections ($X/D=0.6, 0.8, 1$ and 1.2), the stoichiometric case ($\Phi=1$) shows the maximum of NOx because this case develops zones with high temperatures.

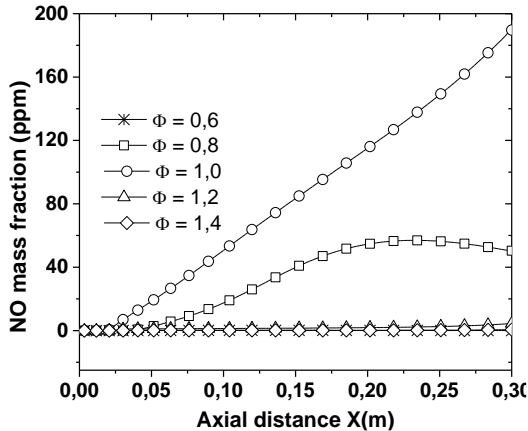


Fig. 17. Thermal NO mass fraction profiles for different CH4 equivalence ratio.

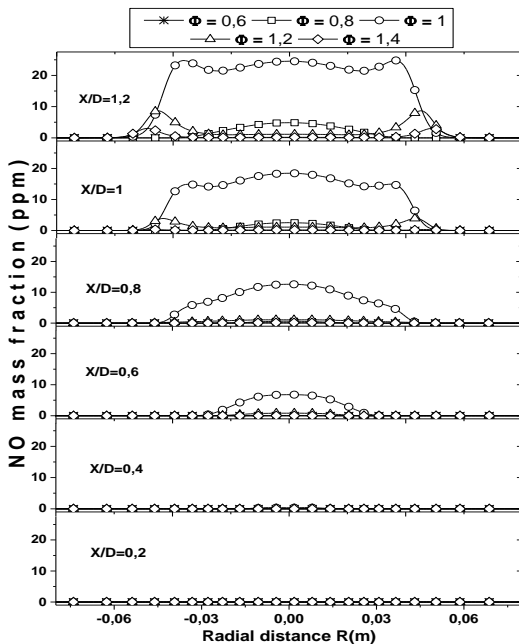


Fig. 18. NO mass fraction profiles for different CH4 equivalence ratios.

The study of the swirl intensity effect illustrated in figure 19 showed that NOx appearance remains negligible for all tested cases (from $S=0.5$ to $S=1.0$). The maximum of NO mass fraction is 0.18, this indicate that the increase of swirl intensity in this type of configuration remains negligible.

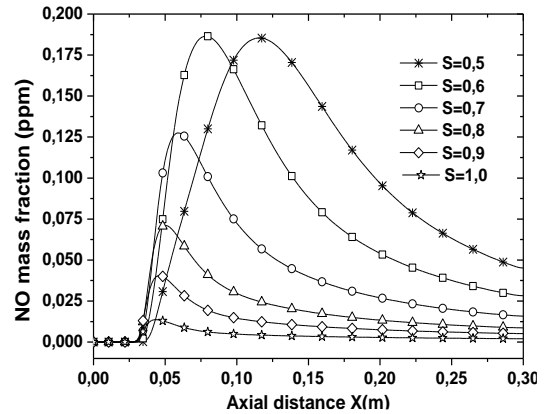


Fig. 19. Thermal NO mass fraction profiles for different swirl number.

5. CONCLUSION

A numerical simulation study of coupled RANS $k-\epsilon$ and Partially Premixed model for methane-air flames with swirl has been developed and validated.

The models haven't shown applicability limit by increasing CH4 equivalence ratio and swirl intensity.

Obtained results were acceptable and proved that the flame is strictly separated from the burner nozzle, thus demonstrating the operating principle of this type of burners (LSB).

Partially premixed combustion model has proven its ability to predict and analyze the distribution of chemical species (CH4 and air) and the appearance of pollutants (Thermal NO).

The turbulence model used (RANS Standard $k-\epsilon$) was able to predict a reasonable flow field of the flame defining its structure. This can be a significant advance in the numerical simulation field considering the time and computing costs, which are less important than means required by the LES and DNS approaches especially for large structures of LSB burners.

The increasing equivalence ratio of CH4 does not affect directly the appearance of thermal NO. However, it showed that the flame front is most significant in the radial distance where the temperature was the most important. Therefore, the flow field may become more sensitive to external flow conditions and consequently increase the risk of dynamic instabilities and extinctions.

The other hand, its augmentation hasn't appear recirculation zones, which shows the importance of LSB burner remaining an excellent alternative for the zero emissions concepts.

The burner exploited in this study was designed for 27 kilowatts of capacity, to increase power; we recommend an increase in global structure of the burner.

The study of swirl intensity shows creation of recirculation zones, but this reduces the flame stabilization but does not increase the creation of NOx produced.

We recommended to use a swirl number lower than 0.6.

REFERENCES

- ANSYS Fluent 14.5 (2012). *Guide theory*.
- Bell, J. B., M. S. Day and J. F. Grac (2002). Numerical simulation of premixed turbulent methane combustion *Proceedings of the Combustion Institute* Volume 29, 1987–1993.
- Bell, J. B., R. K. Cheng, M. S. Day and I. G. Shepherd (2007). Numerical simulation of Lewis number effects on lean premixed turbulent flames. *Proceedings of the Combustion Institute* 31 1309–1317.
- Blauvens, J., B. Smets and J. Peters (1977). 16th Symposium.(Int'l.)on Combustion. The Combustion Institute. Pittsburgh.
- Cheng, R.K. (1995). Velocity and Scalar Characteristics of Premixed Turbulent Flames Stabilized by Weak Swirl. *Combustion and flame* 101, 1-14.
- Cheng, T.S., C.Y. Wu, Y.H. Li and Y.C. Chao (2006). Chemiluminescence measurements of local equivalence ration in a partially premixed flame. *Combust. Sci. and Tech* 178, 1821–1841.
- Chorin, A.J. (1968). Numerical solution of navier-stokes equations. *Mathematics of Computation* 22, 745–762.
- Flower, W.L., R. K. Hanson and C. H. Kruger (1975). 15th Symposium.(Int'l.)on Combustion. The Combustion Institute. 823. Pittsburgh.
- Galpin, J., A. Naudin, L. Vervisch, C. Angelberger, O. Colin and P. Domingo (2008). Large-eddy simulation of a fuel-lean premixed turbulent swirl-burner. *Combustion and Flame* 155 247–266.
- Huang, Y. and V. Yang (2005). Effect of swirl on combustion dynamics in a lean-premixed swirl-stabilized combustor. *Proceedings of the Combustion Institute* 30, 1775–1782.
- Johnsona, M.R., D. Littlejohna, W.A. Nazeerb, K.O. Smithb and R.K. Cheng (2005). A comparison of the flow fields and emissions of high-swirl injectors and low-swirl injectors for lean premixed gas turbines. *Proceedings of the Combustion Institute* 30, 2867–2874.
- Launder, B.E. and D.B. Spalding (1972). Lectures in Mathematical Models of Turbulence. Academic Press, London, England.
- Littlejohn, D., R.K. Cheng, D.R. Noble and L. Tim (2010). Laboratory Investigations of Low-swirl Injectors Operating With Syngases. *Journal of Engineering for Gas Turbines and Power* 132, 011502-1.
- Monat, J.P., R.K. Hanson and C. H. Kruger (1979). 17th Symposium.(Int'l.)on Combustion. The Combustion Institute. 543. Pittsburgh.
- Nogenmyr, K.J., C. Fureby, X.S. Bai, P. Petersson, R. Collin and M. Linne (2009). Large eddy simulation and laser diagnostic studies on a low swirl stratified premixed flame. *Combustion and Flame* 156, 25–36.
- Pesenti, B. (2006). *Caractérisation numérique et expérimentales d'un brûleur à gaz à swirl variable : Longueur le la flamme, Transfert thermique et apparition des NOx*. Ph. D. thesis, Faculté polytechnique de MONS, service de thermique et combustion.
- Petersson, P., R. Wellander, J. Olofsson, H. Carlsson, C. Carlsson, B.B. Watz, N. Boetkjaer, M. Richter, M. Aldén, L. Fuchs and X.S. Bai (2012). Simultaneous high-speed PIV and OH PLIF measurements and modal analysis for investigating flame-flow interaction in a low swirl flame. *16th IntSymp on Applications of Laser Techniques to Fluid Mechanics*, Lisbon, Portugal.
- Pfadler, S., A. Leipertz, F. Dinkelacker, J. Wa'sle, A. Winkler and T. Sattelmayer (2007). Two-dimensional direct measurement of the turbulent flux in turbulent premixed swirl flames. *Proceedings of the Combustion Institute* 31, 1337–1344.
- Plessing, T., C. Kortschik, N. Peters, M.S. Mansour and R.K. Cheng (2000). Measurements of the turbulent burning velocity and the structure of premixed flames on a low swirl burner *Proceedings of the Combustion Institute* Volume 28, 359–366.
- Pope, S.B. (1985). Pdf methods for turbulent reactive flows. *Progress Energy Combustion Science*, 11. 119.
- Truffin, K. (2005). *Simulation aux grandes échelles en identification acoustique des turbines à gaz en régime partiellement pré-mélangé*. Ph. D. thesis, Institut national polytechnique de Toulouse École doctorale: EDYF Spécialité : Dynamique des Fluides. Toulouse. France.
- Vandoormaal, J.P and G.D. Raithby (1984). Enhancements of the SIMPLE Method for Predicting Incompressible Fluid Flows. *Numer. Heat Transfer* 7. 147–163
- Veynante, D. and L. Vervisch (2002). Turbulent combustion modeling. *Progress in energy and combustion Science* 28, 193-266.
- Zimont, V. (2000). Gas Premixed Combustion at High

- Turbulence. Turbulent Flame Closure Model Combustion Model. *Experimental Thermal and Fluid Science* 21.179–186.
- Zimont, V., W. Polifke, M. Bettelini and W. Weisenstein (1998). An Efficient Computational Model for Premixed Turbulent Combustion at High Reynolds Numbers Based on a Turbulent Flame Speed Closure. *Journal of Gas Turbines Power* 120, 526–532.
- Zimont, V.L. and A.N. Lipatnikov (1995). A Numerical Model of Premixed Turbulent Combustion of Gases. *Chem. Phys. Report* 14(7), 993–1025.